# Atomic structure of the cleaved Si(111)−(2×1) surface refined by dynamical LEED

Geng Xu, Bingcheng Deng,* and Zhaoxian Yu
*Department of Physics, Zhongshan University, Guangzhou 510275, China*

S. Y. Tong
*Department of Physics and Materials Science, City University of Hong Kong, Tat Chee Avenue, Kowloon, Hong Kong, China*

M. A. Van Hove
*Materials Sciences Division and Advanced Light Source, Lawrence Berkeley National Laboratory, 1 Cyclotron Road, Berkeley, California 94720, USA*
*and Department of Physics, University of California, Davis, California 95616, USA*

F. Jona
*Department of Material Science and Engineering, S.U.N.Y. at Stony Brook, New York 11794, USA*

I. Zasada
*Solid State Physics Department, University of Lódz, Pomorska 149/153, Lódz, Poland*
(Received 9 March 2004; revised manuscript received 16 April 2004; published 13 July 2004)

Several alternative models have been proposed for the much-studied Si(111)-(2×1) surface structure, including: A reverse-tilted $\pi$-bonded chain model [Zitzlsperger *et al.* Surf. Sci **377**, 108 (1997)]; a three-bond scission model [by Haneman, Phys. Rev. **121**, 1093 (1961)]; and a $\pi$-bonded chain model with enhanced vibrations (present work). These models are compared here to the generally accepted modified $\pi$-bonded chain model [Himpsel *et al.*, Phys. Rev. B. **30**, 2257 (1984)], by analyzing low-energy electron diffraction (LEED) intensity–voltage curves measured earlier. Using the efficient automated tensor LEED technique, the models can be refined to a much greater degree than with earlier methods of LEED analysis. This study distinctly favors the earlier modified $\pi$-bonded chain model, but with strongly enhanced vibrations. To compare models that have different numbers of adjustable free parameters, a Hamilton ratio test is used: It can distinguish between improvement due to a better model and improvement due only to more parameters.

DOI: 10.1103/PhysRevB.70.045307 PACS number(s): 68.35.Bs, 68.47.Fg, 68.49.Jk

## I. INTRODUCTION

The (2×1) reconstruction of the Si(111) surface, prepared by cleaving in an ultrahigh vacuum, was observed more then forty years ago by low-energy electron diffraction (LEED). It was among the very first semiconductor surface structures to be studied in the field of surface science. In 1961, Haneman proposed a buckled model for this surface structure, with alternating outer atoms raised and lowered relative to an ideal bulk termination.[1] Many other structural models were proposed in the next twenty years.[2] In particular, in 1981, Pandey proposed the $\pi$-bonded chain model, after comparing ultraviolet photoemission spectroscopy data and theoretical calculations based on a realistic tight-binding scheme,[3] and then based on a self-consistent pseudo potential method.[4] This model involves a strong rearrangement of bonds in the topmost two atomic layers. Figure 1(a) shows the bulk terminated structure of the Si(111) surface, and Fig. 1(b) shows the Pandey model. The reconstruction moves atom 4 into the surface so it bonds directly to atom 5; atom 1 moves outward and bonds inward to atom 4, removing the dangling bond of atom 4, while creating a dangling bond at atom 1. As a result of the bond rearrangement, atoms 1 and 2 are located at the same height over the surface and form a zigzag chain along the surface. Pandey found that the atoms in the zigzag chain (atoms 1 and 2) form $\pi$-bonds between them.

The $\pi$-bond chain model was largely supported by many subsequent studies, including by total energy calculations,[5,6] ion scattering,[7] optical absorption,[8] electron energy-loss spectroscopy,[9] and photoemission,[10] even though some discrepancies remained between studies.

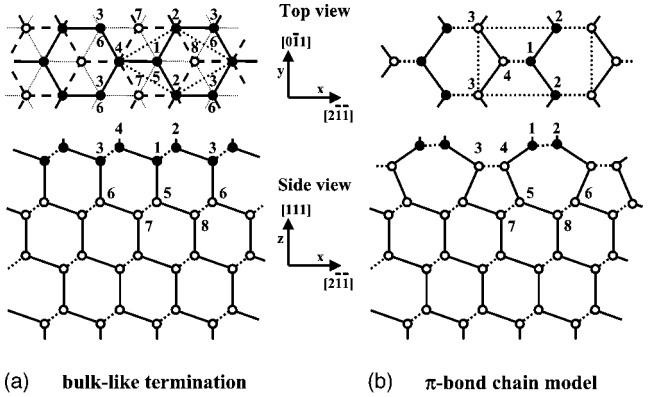


FIG. 1. Si(111) surface: (a) Bulklike termination, in side view and (b) Pandey's $\pi$-bonded chain model, in side and top views. Pandey's model is obtained by switching the bond between atoms 1 and 5 to occur between atoms 4 and 5.

 

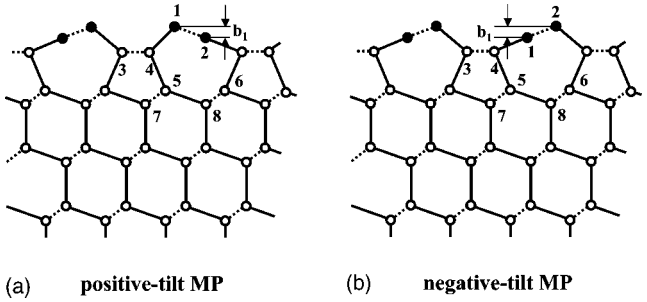


FIG. 2. MP model of Si(111)-(2×1), in side view: Himpsel *et al.*'s modified model (a) with positive tilt (+MP model), as originally proposed, and (b) with negative tilt (−MP model), as supported by total-energy theory.

Himpsel *et al.*, however, showed that the original Pandey model did not meet the LEED test, giving unacceptable disagreement between LEED theory and experiment.[11] In that study, a modified model was proposed and investigated, in which the bonds between the outermost atoms 1 and 2 are tilted (Fig. 2): In this "modified Pandey model" or "MP model", these two atoms are at different heights over the surface. The best fit in that LEED analysis occurred for a positive tilt of $b_1 = 0.38$ *Å* [Fig. 2(a)], but it gave only moderate agreement between experimental and calculated current–voltage (I–V) curves, with a Zanazzi–Jona *R* factor of 0.42. In that analysis, a root mean square (rms) vibration amplitude of 0.1 *Å* was used for all atoms except atoms 1 and 2. The authors noted that a larger surface vibration amplitude (rms = 0.3 *Å*) for these two atoms gave somewhat better visual agreement, but did not change the *R* factor of their optimum structure.

Further studies with LEED (Refs. 12 and 13) and medium-energy ion scattering[14] confirmed the MP model, suggesting values of $b_1 = 0.34$ to 0.40 *Å*. Two theoretical investigations[15,16] supported larger values of $b_1 = 0.47$ to 0.49 *Å*.

Another theoretical study,[17] based on slab-MINDO calculations, showed that the optimization of the total energy with respect to the detailed geometry of this MP model produced two minima differing in energy by 0.006 eV per surface atom. The less stable of these two configurations is characterized by a "positive tilt" of the topmost chain [as in Himpsel *et al.*'s MP model, see Fig. 2(a)], with $b_1 = 0.15$ *Å*: we call this model "+MP". The lowest energy configuration was found to exhibit a "negative tilt" [atom 2 is higher than atom 1, see Fig. 2(b)], with $b_1 = -0.23$ *Å*: We call this model "−MP". Since the energy barrier separating these two configurations is only 0.011 eV per surface atom, it is reasonable to expect the coexistence of both tilt directions at the surface, possibly with thermal flipping between the two structures. A more accurate theoretical calculation based on first principles was performed by Zitzlsperger *et al.*[18] Similar results were obtained, with two minima differing by only 0.0027 eV per surface atom and separated by a barrier of at most 0.037 eV/surface atom; they exhibit larger tilts of $b_1 = 0.44$ *Å* and $b_1 = -50$ *Å* for the positive tilt (second best) and negative tilt (best) configurations, respectively.

Recently, three very different surface structures have emerged from detailed LEED studies which display markedly enhanced surface vibrations (or similar static disorder indicating the coexistence of energetically similar structures): $H_2O$ (0001) (water ice),[19] $Al_2O_3$ (0001),[20] and Ga(010).[21] Each of these exhibits rms vibration amplitudes of the outermost atoms that are about twice as large as in the bulk. A common feature between these structures, which at first sight may appear to be quite disparate, is that the outermost atoms (or molecules in the case of ice) do not have bonds to atoms (or molecules) directly below them within the surface: As with atoms 1 and 2 in Fig. 2, these atoms/molecules are held through bonds that are more parallel to the surface. Such bonds can bend relatively easily (much more easily than bond lengths can be compressed or stretched), allowing these atoms/molecules to vibrate perpendicular to the surface with relatively large amplitudes. A similar geometry exists at the Si(111) surface, including in the MP model: Thus, we propose an MP model with similarly enhanced vibrations.

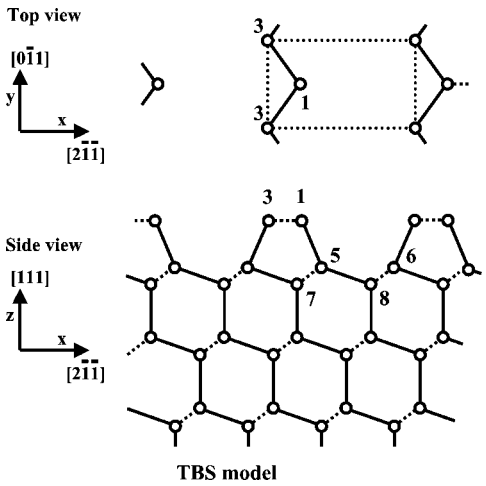


FIG. 3. TBS model, in side and top views. This is obtained from the ideal bulk termination by removing the atoms 2 and 4 in Fig. 1(a), and letting atoms 1 and 3 bond to each other, forming a zigzag chain parallel to the surface.

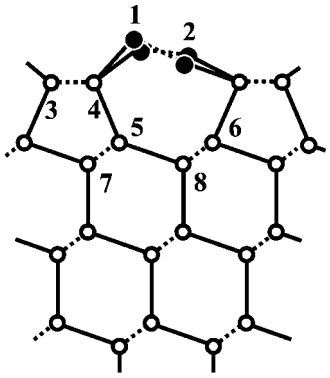


FIG. 4. Split-atom version of MP model of Si(111)-(2×1), in side view: Atoms 1 and 2 are shown split with their optimized positions.

In 1961, Haneman *et al.*, proposed a radically different model for Si(111)-$(2\times1)$: the three-bond scission (TBS) model,[1,22] illustrated in Fig. 3. It was based on a variety of experimental observations, including later data, especially from scanning tunneling microscopy (STM).[23] The TBS model is obtained by a different termination of the bulk Si lattice: Cutting through 3 Si-Si bonds per $(1\times1)$ unit cell instead of through one Si-Si bond, followed by forming new bonds between surface atoms, and resulting in a different kind of zigzag chains along the surface. The authors argued that many observations are incompatible with the MP model, but instead favor the TBS model. On the other hand, Craig and Smith[17] investigated this TBS model and found it to be less favorable than the MP model. Also, a later unpublished LEED analysis found the TBS model to give less good agreement than the MP model.[24]

Prompted by these possibilities for the structure of the Si(111)-$(2\times1)$ surface, and the very modest degree of fit in the last LEED analyses,[11–13] we decided to apply more recent LEED methods to this problem. In addition, a thorough study of this surface would enable the further testing of methods, such as low-energy positron diffraction,[25] for the determination of surface structure.

## II. APPROACH

Our analysis is based on experimental LEED data used in the 1984 analysis:[11] the data set consists of I–V curves for 16 beams (symmetry-reduced to 14 beams with a cumulative energy range of 2147 eV taken at normal incidence at room temperature.

We use the automated tensor LEED method,[26,27] which allows fitting relatively many adjustable fit parameters using an efficient automated search procedure.

In addition, we use the split-atom method[28–30] to describe the large displacements inherent in enhanced vibration amplitudes that extend beyond the validity of the usual Debye–Waller factor. In this approach, an atom that vibrates with a large amplitude is split into several "split atoms" in different positions that approximate the spatial extent of the vibrations (no scattering path is allowed to link the split positions). In our implementation, each split position gives rise to a different surface structure, treated as separate surface domains for which we perform independent LEED calculations: The resulting LEED intensities are then averaged over the intensities from the different structures. In our Si(111)-$(2\times1)$ structure analysis, we split atoms in just two fragments (representing a maximum displacement outward from the surface

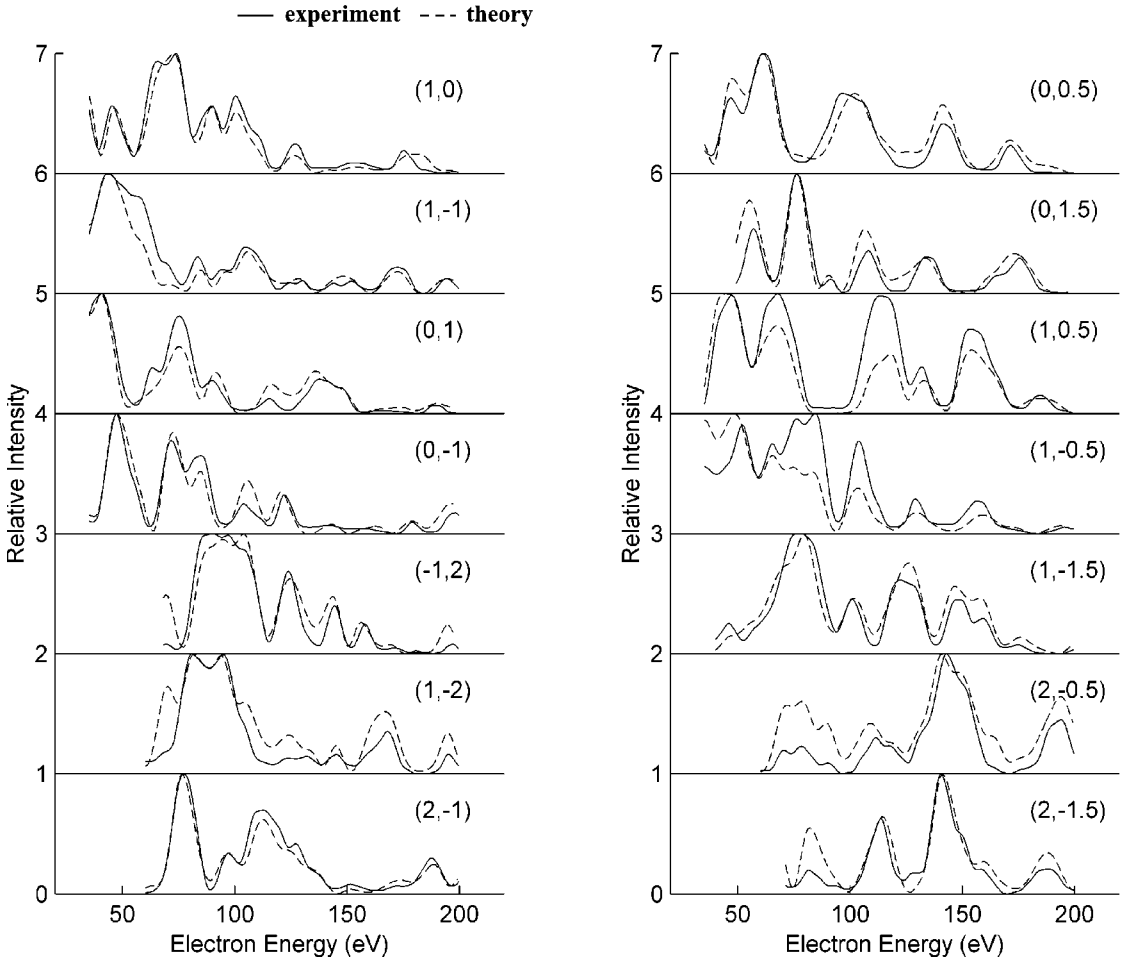


FIG. 5. Experimental and theoretical I–V curves for Si(111)-$(2\times1)$. The experimental I–V curves are shown as full lines. The dashed I–V curves are calculated for the best-fit structure, the MP model structurally optimized with large vibrations.

TABLE I. Comparison of $R$ factors and Hamilton ratios for different structural models of Si(111)-$(2\times1)$, after optimization by automated tensor LEED (the number of optimized parameters is indicated): TBS=three-bond scission model; +MP, −MP=positive-tilt and negative-tilt Modified Pandey models; MP+ split =MP model with split atoms; MP large vibrations=MP model with large vibrations. The optimizations were performed by minimizing each $R$ factor separately. The numbers of parameters shown between parentheses are weighted for depth. The Hamilton ratios are calculated with respect to the MP model, using the $R_{VHT}$ $R$ factor. The Hamilton ratios between parentheses use depth-weighted values $p^*$ and $q^*$ (since the TBS and MP models have the same number of fit parameters, $p=q$, the Hamilton ratio is not defined between them).

| Model | $R$ factors | | | | No. of parameters | Hamilton ratio versus MP |
|---|---|---|---|---|---|---|
| | $R_x(R1)$ | $R_{RZJ}(R8)$ | $R_{PE}(R10)$ | $R_{VHT}(R11)$ | | |
| TBS | 0.316 | 0.321 | 0.462 | 0.308 | 33 | |
| MP | 0.213 | 0.146 | 0.306 | 0.192 | 33 (23) | |
| +MP&−MP | | | | 0.169 | 66 (45) | 0.39 (0.8) |
| MP+split | | | | 0.137 | 66 (46) | 1.30 (2.6) |
| MP large vibrations | 0.143 | 0.124 | 0.158 | 0.151 | 33 (24) | 46 (52) |

and a maximum displacement into the surface), so that we only need to average over pairs of calculated LEED intensities. The average gives the two split positions equal weights, in view of the small difference in the calculated energies between them.

The Si potential was generated using a self-consistent full linearized augmented-plane-wave method[31] in the Si bulk crystal. The phase shifts were then calculated as usual within the muffin-tin approximation, with $I_{\max}=8$[27]. The imaginary part of the potential is set to −3.5 eV. The Debye temperature is initially chosen as $\theta_D=645$ K and the sample temperature is held at 300 K,[32] but the atomic vibration amplitudes were varied in the outermost layers, as described further below.

To gauge the quality of fit between theory and experiment, we applied four different $R$ factors:[33] $R_x$ (=$R1$ in the Van Hove–Barbieri LEED codes,[27] $R_{RZJ}$+(−$R8$), $R_{PE}$(=$R10$), and $R_{VHT}$(=$R11$). $R_X$ compares intensities by integrating over the absolute difference between intensities; $R_{RZJ}$ is the "reduced" Zanazzi–Jona $R$ factor; $R_{PE}$ is the Pendry $R$ factor; and $R_{VHT}$ is the Van Hove–Tong $R$ factor that averages over ten different $R$ factors, including $R_X$, $R_{RZJ}$, and $R_{PE}$.

The coexistence of two different structures on the same surface is handled in our LEED analyses by assuming that diffraction from the two types of structure is incoherent, such that intensities from the separate structures can be added. This also applies to the case of separate structures due to split positions (see above).

To optimize two coexisting structures simultaneously, we apply the following "domain iteration" method. Assuming a 50:50 mix of the two structural domains, we first select a starting structure for each domain, and average their calculated intensities with 50:50 weights. Next, one of the two structures is frozen, while the other is optimized by automated tensor LEED; for this purpose, the varying intensities of the domain being optimized are averaged (50:50) with the constant intensities of the frozen domain. Then, the second domain is frozen, while the first is optimized in the same fashion. This process is repeated until convergence of the results.

One complication in comparing the different models arises from the fact that they have very different numbers of adjustable parameters. This occurs especially with the coexisting structures, which have double the number of free parameters compared to most other models. Clearly, more adjustable parameters allow a better fit, regardless of whether the underlying model is better or worse. To help distinguish a better fit due merely to more fit parameters from a better fit due to an inherently better model, we apply the Hamilton ratio test, common in x-ray diffraction,[34,35] and adapted to LEED.[20] The Hamilton ratio test is based on statistical analysis (ignoring systematic errors). The Hamilton ratio $H$ is defined as

$$H=\frac{R_c^2-R_u^2}{R_u^2}\frac{n-p}{p-q}.$$

Here, $R_c$ is the constrained $R$ factor, obtained for a structure with fewer free parameters $q$, and $R_u$ is the unconstrained $R$ factor, obtained for a structure with more free parameters $p>q$, so that $R_c>R_u$; $n$ is the number of experimental data used. Here, we use the $R_{VHT}$ values to calculate $H$.

In ideal statistical conditions, the Hamilton ratio $H$ should exceed 3 to indicate real improvements, while values below 1 merely indicate a better fit due to more parameters. However, even when a structure passes the Hamilton test, one must still check that the structure is physically reasonable, with acceptable bond lengths and angles.

For LEED, at first, it is not clear what the number of experimental data $n$ should be, since LEED uses continuous curves rather than discrete data points. It has proven adequate to use for $n$ the total number of peaks that can be fit within all experimental I–V curves (summed over symmetry-reduced beams), thus counting peaks as individual data points. Using a typical full peak width of 20 eV, $n$ can then simply be obtained by dividing the total energy range used (summed over independent beams) by this peak width.

Furthermore, one may argue that parameters of deeper-lying atoms should carry a smaller weight than those of surface atoms. In this work, we have therefore also weighted the number of parameters $p$ and $q$ according to the depth of the corresponding atoms. This gives smaller values $p^*$ and $q^*$, counting each atom deeper than the second bi-

TABLE II. The atomic coordinates (in *Å*) of the ideal unreconstructed surface, of the best-fit mix of the atom-split +MP structure (positive-tilt MP model), and of the best-fit enhanced-vibration model. The *z*-axis is perpendicular to the surface (positive outward). The *y* coordinates remain bulklike. The two-dimensional unit-cell vectors are: $(x,y)=(6.65,0)$ and $(0,3.84)$*Å*.

| Atom | Ideal bulk terminated structure | | | Mix of split atoms | | | | | | MP structure with enhanced vibrations | |
|---|---|---|---|---|---|---|---|---|---|---|---|
| | | | | +MP structure first domain | | +MP structure second domain | | Average over both domains | | | |
| | *x* | *y* | *z* | *x* | *z* | *x* | *z* | *x* | *z* | *x* | *z* |
| 1 | 3.325 | 1.920 | 2.351 | 4.381 | 3.562 | 4.329 | 3.381 | 4.355 | 3.472 | 4.338 | 3.452 |
| 2 | 4.434 | 0.000 | 3.135 | 5.592 | 2.944 | 5.409 | 3.001 | 5.501 | 2.973 | 5.443 | 2.954 |
| 3 | 0.000 | 0.000 | 2.351 | 1.140 | 2.227 | 0.956 | 2.223 | 1.048 | 2.225 | 1.019 | 2.213 |
| 4 | 1.108 | 1.920 | 3.315 | 2.422 | 2.171 | 2.487 | 2.149 | 2.455 | 2.160 | 2.430 | 2.145 |
| 5 | 0.000 | 0.000 | 0.000 | 0.078 | −0.028 | 0.165 | 0.010 | 0.122 | −0.009 | 0.072 | −0.017 |
| 6 | 3.325 | 1.920 | 0.000 | 3.215 | −0.038 | 3.359 | −0.081 | 3.287 | −0.060 | 3.269 | −0.073 |
| 7 | 5.542 | 1.920 | −0.784 | 5.526 | −0.658 | 5.440 | −0.669 | 5.483 | −0.664 | 5.466 | −0.670 |
| 8 | 2.217 | 0.000 | −0.784 | 2.292 | −0.948 | 2.216 | −0.995 | 2.254 | −0.972 | 2.256 | −0.997 |
| 9 | 5.542 | 1.920 | −3.135 | 5.618 | −3.025 | 5.576 | −3.049 | 5.597 | −3.037 | 5.610 | −3.049 |
| 10 | 2.217 | 0.000 | −3.135 | 2.243 | −3.223 | 2.226 | −3.262 | 2.235 | −3.243 | 2.213 | −3.258 |
| 11 | 4.434 | 0.000 | −3.919 | 4.637 | −3.882 | 4.417 | −3.895 | 4.527 | −3.889 | 4.477 | −3.911 |
| 12 | 1.108 | 1.920 | -3.919 | 1.112 | −3.928 | 1.203 | −3.970 | 1.158 | −3.949 | 1.100 | −3.971 |
| 13 | 4.434 | 0.000 | −6.270 | 4.498 | −6.278 | 4.490 | −6.262 | 4.494 | −6.270 | 4.478 | −6.287 |
| 14 | 1.108 | 1.920 | -6.270 | 1.126 | −6.272 | 1.189 | −6.338 | 1.158 | −6.305 | 1.127 | −6.324 |
| 15 | 3.325 | 1.920 | −7.054 | 3.338 | −6.976 | 3.294 | −7.009 | 3.316 | −6.993 | 3.299 | −6.998 |
| 16 | 0.000 | 0.000 | −7.054 | 0.010 | −7.051 | 0.010 | −7.065 | 0.010 | −7.058 | 0.014 | −7.058 |

layer with a reduced weight of $\exp(-2d/\lambda)$, where $\lambda=7$ *Å* and *d* is the depth below the deepest atom in the second bilayer.

### III. ANALYSIS OF STRUCTURAL MODELS

Table I compares the different structures under investigation for Si(111)-$(2\times1)$, both with *R* factors and Hamilton ratios (based on the $R_{VHT}$ *R* factor).

All proposed models have a mirror plane symmetry perpendicular to the surface. Therefore, we imposed that the structural optimization maintain this mirror plane in all cases.

In each model, the outermost 16 atoms were allowed to freely relax in two dimensions, one parallel and one perpendicular to the surface (thus respecting the mirror symmetry), giving 32 fit parameters. For the mixed +MP/−*MP* terminations and for the split-atom models, this number is doubled, since two similar domains are then free to independently relax. In addition, there is the fit parameter representing the inner potential (muffin-tin zero). And, in the MP model with enhanced vibrations (treated as large vibrations within the Debye–Waller factor), the vibration amplitude is another fit parameter; this last one is not fit automatically in our automated tensor LEED, but is varied manually using a "grid search".

For each model, several different guessed starting geometries were used, to make sure that the converged results do not depend on the starting geometry. Also, the convergence of the method was checked by iterating the optimization: The result of one optimization was used as the starting geometry of the next optimization (this check is needed because the tensor LEED method gradually loses accuracy away from the initial starting geometry). As a further check on convergence, many of the optimizations were repeated by minimizing each *R* factor separately.

The MP model (with coordinates as determined in 1984,[11] but with our theoretical parameters) yields $R_{VHT}=0.192$ (see Table I). The optimized tilt is $b_1=0.51$ *Å*, close to the result of Northrup *et al.* ($b_1=0.47\pm0.05$ *Å*).[16] However, some important features still are in disagreement between the experimental and theoretical I–V curves.

Table I clearly shows that all *R* factors rule out the TBS model: The difference is too large for additional features like enhanced vibrations to keep the TBS model a viable candidate.

Mixing the +MP (positive tilt) and −MP (negative tilt) models yields an improvement over the MP model: $R_{VHT}=0.169$ (see Table I). However, the Hamilton ratio of 0.39 (or 0.8 if weighted by a depth factor) shows that this apparent improvement is likely only due to the doubling of the number of fit parameters from 33 to 66, and not due to an inherent improvement of the structural model. We conclude that this model is not suitable. The best result for this +MP/−MP mix occurred for $b_1=0.539$ *Å* for the positive-tilt domain, and $b_1=-0.219$ *Å* for the negative-tilt domain. However, the bond lengths are not reasonable in the negative-tilt domain. Also, the $b_1$ values are very different from those predicted in Ref. 18. Our optimized values for $b_1$ in the +MP

TABLE III. Surface bond lengths in the best-fit enhanced-vibration model, compared with the bulk value. Atom numbers refer to Fig. 2(a).

| Atom pair | Bond length (Å) |
|---|---|
| 1-2 | 2.271 |
| 1-4 | 2.313 |
| 2-3 | 2.347 |
| 3-4 | 2.384 |
| 4-5 | 2.371 |
| 3-6 | 2.423 |
| 5-7 | 2.359 |
| 5-8 | 2.277 |
| 6-7 | 2.393 |
| 6-8 | 2.386 |
| Bulk | 2.352 |

and −MP domains are 0.539 and −0.219 Å, respectively, compared with 0.44 and −0.50 Å in Ref. 18.

The MP model with enhanced vibrations was treated in two ways: As split positions (modeled as two separate domains) and as large vibration amplitudes within the Debye–Waller model. The split-atom method gives a significant improvement in the $R$ factor ($R_{VHT}$ improves from 0.192 to 0.137), but the associated Hamilton ratio suggests that this improvement could be due to the doubling of fit parameters alone. The Hamilton ratio values (1.30 and 2.6) are relatively neutral in this regard (Table I). Therefore, we also investigated large vibration amplitudes within the standard approach of a Debye–Waller factor. Although this stretches the domain of validity of the Debye–Waller scheme, we do also find a sizeable improvement in the $R$ factors, e.g., $R_{VHT}=0.151$ (Table I). The associated Hamilton ratio is then very much larger, given that there is only one extra fit parameter. This is strong evidence that the large-vibration model is reasonable.

The coordinates resulting from the different optimizations are listed in Table II, while the corresponding surface bond lengths are shown in Table III.

To further support the validity of the enhancement of vibrations in the MP model, we can compare the amplitude of vibrations obtained from the two approaches. With split positions, and with large amplitudes in the Debye–Waller scheme. The atoms undergoing larger vibrations in these two treatments are the two outermost atoms [1 and 2 in Fig. 2(a)].

In the split-atom model, illustrated in Fig. 4, we found a spacing (perpendicular to the surface) between optimum split positions of 0.18 and −0.06 Å for atoms 1 and 2, respectively, giving a full range of deviations of 0.24 Å. These 2 atoms have optimum rms vibration amplitudes of 0.22 Å.

With large vibrations, we found an optimum for an rms amplitude of 0.25 Å (compared to about 0.11 Å in the bulk). The best-fit I–V curves, using the large-vibration model, are shown in Fig. 5. The rms amplitude of 0.25 Å is close to the 0.22–0.24 Å values found for the split positions. In fact, a Gaussian of 0.25 Å width (in the direction perpendicular to the surface) is almost identical to the sum of two Gaussians of width 0.22 Å separated by 0.24 Å. This result suggests that the vibration amplitudes of these two atoms are anisotropic, in contrast to the single MP model with isotropic vibration amplitudes of 0.25 Å. Also significant is that the midpoints of the split positions lie very close to the centers of the optimized large-vibration positions. In addition, we find that the value of $b_1$ obtained with large vibrations (50 Å) lies exactly midway between the two values of $b_1$ found with split positions (0.62 and 0.38 Å). These facts indicate that the two representations are equivalent in terms of describing the extent of the vibrations.

Furthermore, deeper atoms (below atoms 1 and 2) are not noticeably split (split distance $\ll$0.11 Å=rms bulk vibration amplitude). This is an important observation because our approach to the split-position method creates two "domains" in which the atoms are completely free to move independently as far as they need in order to improve agreement with the LEED experiment. The nonsplitting of deeper atoms thus suggests that the default Debye–Waller treatment of their vibrations is sufficient to properly describe them.

## IV. CONCLUSIONS

By applying automated tensor LEED, we are able to test structural models in greater detail than before, optimizing more parameters. By this method, we have considered several alternative models for the Si(111)-(2×1) surface. However, the Three-Bond-Scission model[1,22] can be ruled out.

The negative-tilt model, mixed with the commonly accepted positive-tilt model, improves the agreement between theory and experiment somewhat, but this improvement is likely due only to the doubling of the number of fit parameters: It is thus also disfavored.

We obtain convincingly better agreement by allowing enhanced vibrations of the outermost two atoms. The rms vibration amplitude optimizes to about 0.25 Å, more than double the bulk value. It must be stressed that LEED cannot easily distinguish between vibrational motion and static disorder, so some form of static disorder cannot be excluded. However, it is not clear what kind of static disorder to propose for this surface, and we thus favor dynamic vibrations of large amplitude.

Similar enhanced vibration amplitudes have been observed by similar LEED analyses of three other surface structures that have a common characteristic. The outermost atoms do not form bonds perpendicular to the surface, but nearly parallel to the surface, thereby allowing large bond bending.

## ACKNOWLEDGMENTS

This work was supported in part by the Director, Office of Science, Office of Basic Energy Sciences, Division of Materials Sciences and Engineering, of the U.S. Department of Energy under Contract No. DE-AC03-76SF00098, and by the Research Grants Council of the Hong Kong Special Administrative Region, China, Project No. CityU 1238/02P.

*Permanent address: Department of Basic Courses, South China Construction College, Guangzhou University, Guangzhou 510405, China.

[1] D. Haneman, Phys. Rev. **121**, 1093 (1961).
[2] See, for example, D. J. Chadi, Phys. Rev. Lett. **41**, 1062 (1978).
[3] K. C. Pandey, Phys. Rev. Lett. **47**, 1913 (1981).
[4] K. C. Pandey, Phys. Rev. Lett. **49**, 223 (1982).
[5] J. E. Northrup and M. L. Cohen, Phys. Rev. Lett. **49**, 1349 (1982).
[6] O. H. Nielsen, R. M. Martin, D. J. Chadi, and K. Kunz, J. Vac. Sci. Technol. B **1**, 714 (1983).
[7] R. M. Tromp, L. Smit, and J. F. van der Veen, Phys. Rev. Lett. **51**, 1672 (1983).
[8] P. Chiaradia, A. Cricenti, S. Selci, and G. Chiarotti, Phys. Rev. Lett. **52**, 1145 (1984).
[9] R. Matz, H. Lüth, and A. Ritz, Solid State Commun. **46**, 343 (1983).
[10] R. I. G. Uhrberg, G. V. Hansson, J. M. Nicholls, and S. A. Flodström, Phys. Rev. Lett. **48**, 1032 (1982).
[11] F. J. Himpsel, P. M. Marcus, R. Tromp, I. P. Batra, M. R. Cook, F. Jona, and H. Liu, Phys. Rev. B **30**, 2257 (1984).
[12] R. Feder and W. Mönch, Solid State Commun. **50**, 311 (1984).
[13] H. Sakama, A. Kawazu, and K. Ueda, Phys. Rev. B **34**, 1367 (1986).
[14] R. M. Tromp, L. Smit, and J. F. van der Veen, Phys. Rev. B **30**, 6235 (1984).
[15] F. Ancilotto, W. Andreoni, A. Selloni, R. Car, and M. Parrinello, Phys. Rev. Lett. **65**, 3148 (1990).
[16] J. E. Northrup, M. S. Hybertsen, and S. G. Louie, Phys. Rev. Lett. **66**, 500 (1991).
[17] B. I. Craig and P. V. Smith, Surf. Sci. **225**, 225 (1990).
[18] M. Zitzlsperger, R. Honke, P. Pavone, and U. Schröder, Surf. Sci. **377**, 108 (1997).
[19] N. Materer, U. Starke, A. Barbieri, M. A. Van Hove, G. A. Somorjai, G.-J. Kroes, and C. Minot, J. Phys. Chem. **99**, 6267 (1995); Surf. Sci. **381**, 190 (1997).
[20] C. F. Walters, K. F. McCarty, E. A. Soares, and M. A. Van Hove, Surf. Sci. **464**, L732-8 (2000); E. A. Soares, M. A. Van Hove, C. F. Walters and K. F. McCarty, Phys. Rev. B **65**, 195405 (2002).
[21] S. Moré, E. A. Soares, M. A. Van Hove, S. Lizzit, A. Baraldi, Ch. Grütter, J. H. Bilgram and Ph. Hofmann, Phys. Rev. B **68**, 075414 (2003).
[22] D. Haneman, Rep. Prog. Phys. **50**, 1045 (1987).
[23] I. Andrienko and D. Haneman, J. Phys.: Condens. Matter **11**, 8437 (1999).
[24] A. Kawazu (private communication).
[25] S. Y. Tong, Surf. Rev. Lett. **7**, 21 (2000).
[26] P. J. Rous, and J. B. Pendry, Surf. Sci. **219**, 355 (1989); M. A. Van Hove, W. Moritz, H. Over, P. J. Rous, A. Wander, A. Barbieri, N. Materer, U. Starke, and G. A. Somorjai, Surf. Sci. Rep. **19**, 191 (1993).
[27] A. Barbieri and M. A. Van Hove (http://electron.lbl.gov/leedpack/)
[28] T. Hertel, H. Over, H. Bludau, M. Gierer, and G. Ertl, Phys. Rev. B **50**, 8126 (1994).
[29] H. Over, W. Moritz, and G. Ertl, Phys. Rev. Lett. **70**, 315 (1993).
[30] H. Over, M. Gierer, H. Bludau, and G. Ertl, Phys. Rev. B **52**, 16812 (1995).
[31] E. Wimmer, H. Krakauer, M. Weinert, and A. J. Freeman, Phys. Rev. B **24**, 864 (1981); H. J.F. Jansen and A. J. Freeman, *ibid.* **30**, 561 (1984).
[32] M. A. Van Hove and S. Y. Tong, *Surface Crystallography by LEED* (Springer, Berlin, 1979), p. 30.
[33] M. A. Van Hove, S. Y. Tong, and M. H. Elconin, Surf. Sci. **64**, 85 (1977); M. L. Xu and S. Y. Tong, Phys. Rev. B **31**, 6332 (1985).
[34] W. C. Hamilton, *Statistics in Physical Science* (Ronald Press, New York, 1964).
[35] W. C. Hamilton, Acta Crystallogr. **18**, 502 (1965).